PHYSICAL REVIEW E **72**, 025301(R) (2005)

Droplet motion driven by surface freezing or melting: A mesoscopic hydrodynamic approach

Arik Yochelis[1,*] and Len M. Pismen[1,2,†]
[1]*Department of Chemical Engineering, Technion—Israel Institute of Technology, 32000 Haifa, Israel*
[2]*Minerva Center for Nonlinear Physics of Complex Systems, Technion—Israel Institute of Technology, 32000 Haifa, Israel*
(Received 6 April 2005; published 30 August 2005)

A fluid droplet may exhibit self-propelled motion by modifying the wetting properties of the substrate. We propose a model for droplet propagation upon a terraced landscape of ordered layers formed as a result of surface freezing driven by the contact angle dependence on the terrace thickness. Simultaneous melting or freezing of the terrace edge results in a joint droplet-terrace motion. The model is tested numerically and compared to experimental observations on long-chain alkane systems in the vicinity of the surface melting point.

DOI: 10.1103/PhysRevE.72.025301 PACS number(s): 47.20.Ma, 68.15.+e, 68.08.−p, 83.80.Xz

Motion of mesoscopic liquid droplets is a challenging problem both in view of numerous technological applications in surface treatment, microfluidics, etc., and fundamental questions arising on the borderline between macroscopic and molecular physics. Different scenarios of droplet motion are determined by liquid-substrate interactions, and may incorporate surface phase transitions and chemical reactions, as well as more subtle modification of physical properties in interfacial regions. One can distinguish between three classes of behavior: *passive*, *interacting*, and *active*. A *passive* droplet gains mobility due to imposed forces, e.g., temperature gradients [1] or substrate heterogeneity [2]. Motion of *interacting* droplets is mediated by fluxes through a thin precursor layer [3,4]. Finally, *active* droplets may propel themselves by modifying the substrate either through surfactant deposition at the three-phase contact line [5] or through chemical reaction proceeding directly on the substrate at the foot of the droplet [6,7].

A new type of self-propelled motion discovered recently in experiments with long-chain alkanes (C_nH_{2n+2}) [8] is associated with surface phase transitions creating a terraced immobilized layer between the fluid and substrate, as shown schematically in Fig. 1. The system includes (a) a disordered bulk liquid alkane droplet; (b) one or more ordered (smectic A) alkane layers formed as a result of surface freezing; and (c) a molecularly thin disordered precursor layer. The thickness ratio $l/d \gg 1$ of the smectic and precursor layers is determined by the aspect ratio of the alkane molecule. The plateau height is $H=Nl$, where $N \geqslant 1$ is an integer. A similar situation may arise in layered adsorption, leading to the formation of ordered immobilized molecular layers with the aspect ratio $l/d \sim \mathcal{O}(1)$.

Due to a difference in molecular interaction strengths between the bulk fluid and the smectic and the substrate, the contact angle of the bulk droplet depends on the number of smectic layers, and, therefore, the droplet is expected to move when placed on a terrace as in Fig. 1. Moreover, as temperature is varied, the terrace surface freezing process may proceed in two ways, depending on whether it is limited by material supply or removal of latent heat. The first mechanism involves slow spreading, with the smectic layer growing sidewise, being augmented by fluid molecules migrating from the bulk droplet through the precursor [9]. The second mechanism is fast, and involves terrace growth synchronous with the droplet motion [8]. Melting, being unconstrained by material supply, proceeds by the second mechanism in reverse. In this Rapid Communication, we suggest a model of self-propelled droplet motion accompanied by surface freezing or melting on a terraced landscape.

We adopt the lubrication approximation, which accounts for different scalings in the vertical and the horizontal directions [10]. The approximation is applicable in a liquid film with a large aspect ratio, when the interface is weakly inclined and curved. The scaling is consistent if one assumes $\partial_z \sim \mathcal{O}(1)$, $\nabla \sim \mathcal{O}(\epsilon) \ll 1$, $\partial_t \sim \mathcal{O}(\epsilon^2)$, where ∇ is the two-dimensional gradient in the horizontal plane. This scaling also implies a small contact angle, $\theta \sim \mathcal{O}(1)$ and results in a different order of magnitude of the vertical and horizontal velocities, $v_z \sim \mathcal{O}(\epsilon^2)$, $v_x \sim v_y \sim \mathcal{O}(\epsilon)$. As a consequence, the pressure or, more generally, a driving potential W is constant to $\mathcal{O}(\epsilon^2)$ across the layer in z direction. The governing equation for the droplet height h following the mass conservation condition reads

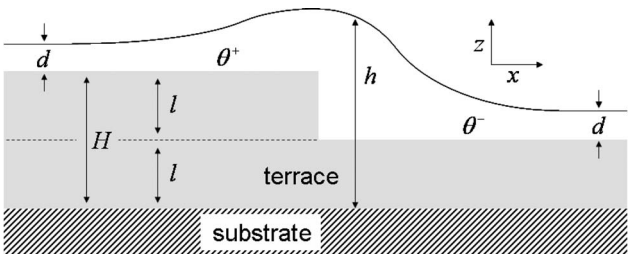

FIG. 1. A scheme of a droplet on a terraced smectic layer. l and d denote, respectively, the molecular dimensions along and across the long molecular axis; $H=Nl$ is the terrace height, N is an integer that denotes the number of layers, h is the bulk droplet height, and $\theta^{\pm}$ are the contact angles on the upper and lower plateaus.

*Electronic address: yochelis@technion.ac.il
†Electronic address: pismen@technion.ac.il

$$\partial_t h = -\nabla \cdot \mathbf{j}, \quad \mathbf{j} = -\eta^{-1} k(h) \nabla W, \quad W = \Pi - \sigma \epsilon^2 \nabla^2 h, \tag{1}$$

where $\mathbf{j}$ is the mass flux, η is the dynamic viscosity, $k(h)$ is the mobility coefficient, σ is the surface tension, and Π is the disjoining potential due to interaction with the solid support (including both substrate and smectic layers).

Computation of Π is the key component of the model. We assume that all interactions are of the van der Waals type with the hard-core potential $V(r)=\infty$ at $r<d$, $V(r)=-A_j r^{-6}$ at $r>d$, and differ by interaction constants A_j only. Since the motion is, on the one hand, caused by the difference in contact angles on the two sides and, on the other side, is driven by excess free energy of either freezing or melting, the difference between the liquid-terrace (A_t) and liquid-substrate (A_s) interaction constants should change sign when the temperature passes the surface melting point. Equilibrium contact angles can be expressed through the interaction constants by integrating Eq. (1) for an infinite bulk fluid in equilibrium as explained below.

For a fluid on top of a flat homogeneous plateau, $z>H$ (see Fig. 1), the free energy per unit area can be written, in a local density-functional approximation [11], as

$$\gamma = \int_H^\infty n(z) \Bigg\{ f(n) - \int_{-\infty}^H Q(z-\zeta) n(z) d\zeta + \frac{1}{2} \int_H^\infty Q(z-\zeta)[n(\zeta) - n(z)] d\zeta + \alpha_t n_t \int_0^H Q(z-\zeta) d\zeta + \alpha_s n_s \int_{-\infty}^0 Q(z-\zeta) d\zeta \Bigg\} dz. \tag{2}$$

Here $n(z)$, n_t, n_s are the fluid, terrace, substrate particle densities, and $f(n)$ is free energy per particle of a homogeneous fluid. The first term in the integrand is the free energy per particle in the homogeneous fluid; the second term compensates lost fluid-fluid interactions in the domain $z<H$ which are included in $f(n)$; the third term accounts for the inhomogeneous part of fluid-fluid interactions; the last two terms represent the fluid-terrace and fluid-substrate interactions. All interactions are described by the same hard-core interaction potential differing only by interaction strength, A (fluid-fluid), $A_t=\alpha_t A$ (fluid-terrace), and $A_s=\alpha_s A$ (fluid-substrate). The interaction kernel $Q(\zeta)$ lumping intermolecular interaction between the layers z=constant [11] is expressed then as $Q(\zeta)=\frac{1}{2}\pi A \zeta^{-4}$ at $\zeta>d$.

Since the precursor layer is of molecular thickness, the chemical potential shift is computed differently in the bulk and precursor regions; this is unlike other self-propelled active drop models [7] where a macroscopic precursor layer was presumed. In the *bulk* region $z>H+d$ the chemical potential shift $\mu(h)-\mu_0$ from the equilibrium value in the bulk fluid, $\mu=\mu_0$, depends on the fluid thickness h and coincides with the disjoining potential, $\Pi(h)=\partial_h \gamma$ [12]. Neglecting the vapor density, as well as density variation in a molecularly thin interfacial layer, we can apply the sharp interface approximation [13], assuming the fluid density to be constant, $n=n_0$ at $H+d<z<h$, where n_0 is the equilibrium fluid particle density at $\mu=\mu_0$, $n=0$ at $z>h$. Defining $\hat{\gamma}(h)$ by Eq. (2) with the upper integration limit over z replaced by h and the homogeneous part excluded, we compute

$$\Pi(h) = \frac{\partial \gamma}{\partial h} = -\frac{\pi A n_0^2}{6} \left[\frac{\chi}{(h-H)^3} + \frac{\chi_\alpha}{h^3} \right], \tag{3}$$

where $\chi=\alpha_t n_t/n_0-1$ and $\chi_\alpha=(\alpha_s n_s-\alpha_t n_t)/n_0$ are dimensionless Hamaker constants for fluid-terrace and terrace-substrate interfaces.

The *precursor* film is assumed to be of a *constant* molecular thickness d, but the liquid density is allowed to vary there, and is determined by minimizing the grand ensemble thermodynamic potential $\mathcal{F}=\gamma-\mu\int n dz$. The disjoining potential is identified here with the shift of the chemical potential per unit volume $\Pi(n)=n[\mu(n)-\mu_0]$ relative to the equilibrium value μ_0 as a function of the local value of n (shifted from its bulk equilibrium value under the action of the terrace and substrate). It is determined by the Euler-Lagrange equation derived from the integrand of (2) for $z=H+d$:

$$\Pi = n\frac{d(nf)}{dn} - n\mu_0 - \frac{\pi A n}{6} \left[\frac{n_0(\chi+1)-n}{d^3} + \frac{\chi_\alpha n_0}{(H+d)^3} \right]. \tag{4}$$

The mobility coefficient $k(h)$ is also computed separately in the *bulk* and *precursor* regions and matched at the precursor thickness. In the bulk region, Stokes flow with a kinematic slip condition [14] is assumed, while in the precursor domain the mass transport is presumed to be purely diffusional. This yields the mobility coefficient [14]

$$k(h) = \begin{cases} \lambda^2 (h-H) + \frac{1}{3}[h-(H+d)]^3 & \text{at } h > H+d; \\ \lambda^2 d & \text{at } h \leqslant H+d, \end{cases} \tag{5}$$

where $\lambda=\sqrt{D\eta/n_0 k_B T}\sim\mathcal{O}(d)$ is the effective slip length; D is the surface diffusivity, k_B is the Boltzmann constant, and T is the temperature.

The motion of a droplet placed on terraced landscape as in Fig. 1 can be attributed to a difference in equilibrium contact angles at the upper (H^+) and lower (H^-) terraces. The rescaled angles can be calculated for $\chi<0$, $|\chi|\ll 1$ by integrating the static equation $W=0$ [11], which reduces to $\sigma\epsilon^2 h_{xx}=\Pi$. In the limit $h\to\infty$ we obtain

$$\theta^\pm = \sqrt{\frac{2}{\epsilon^2\sigma}\int_{h_0}^\infty \Pi dh} = \sqrt{\frac{\pi A n^2 |\chi|}{\epsilon^2 6\sigma d^2}} \sqrt{1 - \frac{\chi_\alpha/|\chi|}{(1+H^\pm/d)^2}}, \tag{6}$$

where $h_0\approx H^\pm+d$. The direction of the droplet motion is determined solely by the effective terrace–substrate interaction, i.e. by the sign of χ_α: the droplet either ascends for $\chi_\alpha>0$ or descends for $\chi_\alpha<0$ until equilibrium is reached. The equilibrium condition $\theta^+=\theta^-$ is satisfied either by $H^+=H^-$ or $\chi_\alpha=0$. The formal small parameter of the lubrication approximation can be defined by setting $\theta=1$ for $\chi_\alpha=0$, which yields $\epsilon\sim\sqrt{|\chi|An^2/(\sigma d^2)}$. Since $\sigma\sim n^2 A/d^2$, a good estimate is $\epsilon\sim\sqrt{|\chi|}$.

A decrement of contact angles should be preserved to maintain droplet propagation. This is possible when the terrace edge is also allowed to move. The terrace motion due to

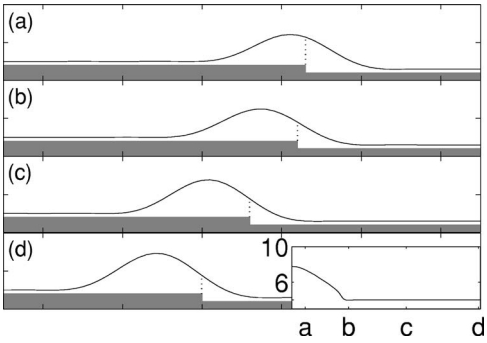

FIG. 2. Numerical solution of the fluid and the terrace according to Eq. (8), showing the melting process (a–d) at respective time steps (from top to bottom: 50, 210, 400, and 650). The horizontal range is $\xi=[0,120]$ and the vertical range is $\hat{h}=[0,20]$. The dotted line marks the droplet height above the terrace edge, $\hat{h}_c$. The inset shows the dependence of $\hat{h}_c-H^+$ as a function of time and its relaxation to an equilibrium value $\hat{h}_c-H^+\simeq 4$. Parameters: $\chi=-0.3$, $\beta=15$, $\lambda=\sqrt{3}$, $l=2$, $H^+=2l$, $H^-=l$, $\chi_\alpha=-10$, and $\Delta=-4$.

surface freezing or melting was observed in the experiment [8] when ambient temperature T was varied in the vicinity of the surface freezing point T_m. When the terrace is at the foot of a liquid droplet, the melting or freezing rate is limited by the heat flux q required to supply or remove the latent heat L, so that $L\rho v=q\approx\mathcal{K}(T-T_m)/(h-H^+)$, where $\mathcal{K}$ is thermal conductivity and ρ is density (assumed to be equal for both liquid and the frozen terrace layer). The approximate expression for the heat flux (directed almost normally to the substrate or terrace) corresponds to the lubrication approximation. The form of this relation defining the edge position x is

$$v=\frac{dx}{dt}=\frac{\mathcal{K}(T-T_m)}{L\rho(h-H^+)}. \tag{7}$$

To reproduce joint droplet-terrace dynamics observed in [8], we have carried out dimensionless one-dimensional (1D) numerical computations of Eqs. (1) and (7). The new dimensionless variable forms are $\hat{h}=h/d$, $\xi=x\epsilon/d$, $\tau=t\epsilon^4\sigma/(d\eta)$, and $\hat{\Pi}=\Pi d/(\epsilon^2\sigma)$. The particle densities are scaled by $1/b$, where $b=2\pi d^3/3$ is the excluded volume so that the respective dimensionless equations are

$$\partial_\tau\hat{h}=-\partial_\xi k(\hat{h})\partial_\xi(\partial_{\xi\xi}\hat{h}-\hat{\Pi}), \tag{8a}$$

$$\hat{v}=\frac{d\xi}{d\tau}=\frac{\Delta}{\hat{h}-H^+}, \tag{8b}$$

where

$$\hat{\Pi}=-\frac{\beta\hat{n}_0^2}{4}\left[\frac{\chi}{(\hat{h}-H)^3}+\frac{\chi_\alpha}{\hat{h}^3}\right]\quad \text{at } \hat{h}>H+1;$$
$$-\frac{\beta\hat{n}}{4}\left[\hat{n}_0(\chi+1)-\hat{n}+\frac{\hat{n}_0\chi_\alpha}{(1+H)^3}\right]-\hat{n}\hat{\mu}_0+\frac{\hat{n}}{1-\hat{n}}$$
$$-\hat{n}\ln\left(\frac{1}{\hat{n}}-1\right)-2\beta\hat{n}^2\quad \text{at } \hat{h}\leqslant H+1, \tag{8c}$$

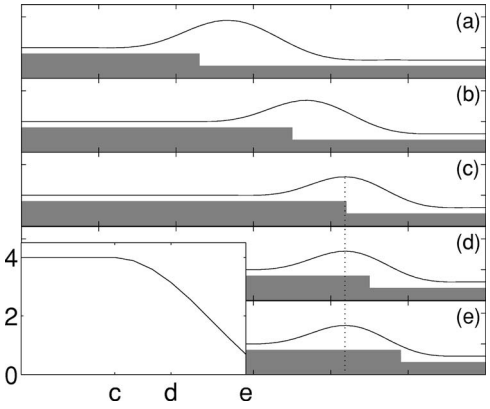

FIG. 3. Numerical solution of Eq. (8), showing the freezing process (a–e) at respective time steps (from top to bottom: 0, 410, 581.85, 581.88, and 581.92). The horizontal range is $\xi=[0,120]$ and the vertical range is $\hat{h}=[0,12]$. The dotted line in (c–e) marks the droplet position according to its maximal height. The inset shows the dependence of $\hat{h}_c-H^+$ on time in the vicinity of the critical droplet volume. Parameters: $\chi=-0.3$, $\beta=15$, $\lambda=\sqrt{3}$, $l=2$, $H^+=2l$, $H^-=l$, $\chi_\alpha=1.5$, and $\Delta=4$.

$$\Delta=\frac{\mathcal{K}(T-T_m)}{L\rho d}\frac{d\eta\epsilon}{\epsilon^4\sigma d}\sim\frac{\mathcal{K}(T-T_m)\eta}{L\rho d\sigma|\chi|^3}, \tag{8d}$$

$\beta=A/(k_BTd^6)$ and $\hat{\mu}_0=\mu_0 b/(k_BT)$. The same notation is retained for the dimensionless variables, and Eq. (5) remains without change, except for replacing $d\to 1$. The density in the precursor domain $\hat{n}$ is transformed to effective height as $\hat{n}=\hat{n}_0(\hat{h}-H)$. We adopted the explicit spectral method; the reflecting boundary conditions are imposed by doubling the grid size. The initial state in each computation includes a droplet with its maximum placed above the terrace edge and a precursor film of unit thickness (see Fig. 1). The parameter Δ defining the ratio of characteristic velocities of the edge to droplet motion is of $\mathcal{O}(1)$ when the temperature difference is in the range of $\mathcal{O}(10^{-3})$ (K).

Synchronous droplet-terrace motion under melting conditions is shown in Fig. 2. This joint propagation can be explained in terms of terminal velocity of the terrace. While the terrace is below the droplet, the droplet velocity is determined by the difference in contact angle values, according to (6). On the other hand, the terrace velocity (for a fixed Δ) depends solely on the thickness of the liquid layer above the terrace edge. At the start, the droplet moves to the left, while the terrace remains almost stationary because of slow transport through a thick layer, as shown Fig. 2(a) and 2(b). As the fluid height above the edge decreases, the terrace gains speed [see Fig. 2(b) and 2(c)], until it reaches an "equilibrium" position, such that the point at the droplet interface just above the edge where the thickness is $\hat{h}_c$ moves with the same speed $\hat{v}=\Delta/(\hat{h}_c-H^+)$. The stable position should lie near the trailing edge; then, if the terrace moves faster than the droplet, the liquid layer thickness above it increases and the terrace decelerates. As a result, the value $\hat{h}=\hat{h}_c$ remains constant, as seen in Fig. 2(c) and 2(d) and more precisely in

inset of Fig. 2(d). This dynamic feedback allows the droplet and the terrace to synchronize their motion. As implied by (6), we found that the synchronous propagation velocity depends on the layers thickness $H^+=Nl$ and will be discussed elsewhere [15].

In the freezing case, the droplet volume decreases, since the total mass of the system is conserved and the fluid is solidified. The droplet and the terrace may still jointly propagate as long as the droplet height is relatively large compared to the precursor thickness, as shown in Fig. 3(a)–3(c). In a such motion the droplet and the terrace preserve the equilibrium height $\hat{h}=\hat{h}_c$ [see Fig. 3(b) and 3(c)]. As the droplet volume decreases below the equilibrium height $\hat{h}_c$, the terrace propagates faster than the droplet and runs out to its leading edge [see Fig. 3(d) and 3(e)]. Following this, the motion stops, since further terrace propagation is limited by slow material supply through the precursor, and the droplet is left in an equilibrium state on the top of a flat smectic layer [8]. This behavior is also presented in the inset of Fig. 3. As the terrace passes the maximum droplet's height, the critical value $\hat{h}_c-H^+$ decreases to unity (i.e., the precursor thickness). The droplet velocity at the same time drops to zero, while the terrace velocity (dashed line) jumps abruptly. Similar behavior has been also observed experimentally [9].

We have proposed a model for self-propelled droplets on top of a terraced landscape driven by surface freezing or melting. The numerical estimates show the characteristic terrace edge velocity $v\sim\mathcal{O}(10^2)[\mu\mathrm{m/sec}]$ close to the experimental data [8] at temperature variations around the surface melting temperature $|T-T_m|\sim\mathcal{O}(10^{-3})$ (K) and $h_c\sim\mathcal{O}(d)\sim 0.1$ (nm).

We thank Hans Riegler for stimulating discussions and for sharing with us his unpublished material. This research has been supported by Israel Science Foundation (Grant No. 55/02) and one of us (A.Y.) also acknowledges the support of Israel Council for Higher Education.

[1] F. Brochard, Langmuir **5**, 432 (1989); M. G. Velarde, Philos. Trans. R. Soc. London, Ser. A **356**, 859 (1998).

[2] E. Raphaël, C. R. Acad. Sci., Ser. II: Mec., Phys., Chim., Sci. Terre Univers **306**, 751 (1988); M. K. Chaudhury and G. M. Whitesides, Science **256**, 1539 (1992).

[3] L. M. Pismen and Y. Pomeau, Phys. Fluids **16**, 2604 (2004).

[4] A. Marmur and M. D. Lelah, J. Colloid Interface Sci. **78**, 262 (1980).

[5] A. Y. Rednikov, Y. S. Ryazantsev, and M. G. Velarde, Phys. Fluids **6**, 451 (1994); A. S. Mikhailov and D. Meinköhn, in *Lecture Notes in Physics*, edited by L. Schimansky-Geier and T. Pöschel (Springer, Berlin, 1997), Vol. 484, p. 334.

[6] C. D. Bain, G. D. Burnetthall, and R. R. Montgomerie, Nature (London) **372**, 414 (1994); F. Domingues Dos Santos and T. Ondarcuhu, Phys. Rev. Lett. **75**, 2972 (1995); S. W. Lee, D. Y. Kwok, and P. E. Laibinis, Phys. Rev. E **65**, 051602 (2002).

[7] U. Thiele, K. John, and M. Bär, Phys. Rev. Lett. **93**, 027802 (2004).

[8] P. Lazar and H. Riegler, Phys. Rev. Lett. (to be published).

[9] P. Lazar, H. Schollmeyer, and H. Riegler, Phys. Rev. Lett. **94**, 116101 (2005).

[10] A. Oron, S. H. Davis, and S. G. Bankoff, Rev. Mod. Phys. **69**, 931 (1997).

[11] L. M. Pismen, Phys. Rev. E **64**, 021603 (2001); A. Yochelis and L. M. Pismen (unpublished).

[12] B. V. Derjaguin, N. V. Churaev, and V. M. Muller, *Surface Forces* (Consultants Bureau, New York, 1987).

[13] S. Dietrich and M. Napiórkowski, Phys. Rev. A **43**, 1861 (1991).

[14] L. M. Pismen and B. Y. Rubinstein, Langmuir **17**, 5265 (2001).

[15] A. Yochelis, E. Knobloch, and L. M. Pismen (unpublished).